Supporting Information

Super-Stable Cu(I)-Based Polymer Exhibiting Thermally Activated Delayed Fluorescence and Water/Acid-Resistant Properties

Yue Wu,[*a] Xin Zhang,[a] Xiao-Meng Zhen,[a] Yan Yang,[a] Bo Zhang[*a] and Jun Li[*a]*

E-mail: ywu_lcu@163.com

[a] College of Chemistry and Chemical Engineering, Shandong Provincial Key Laboratory/Collaborative Innovation Center of Chemical Energy Storage and Novel Cell Technology, Liaocheng University, Liaocheng 252059, China

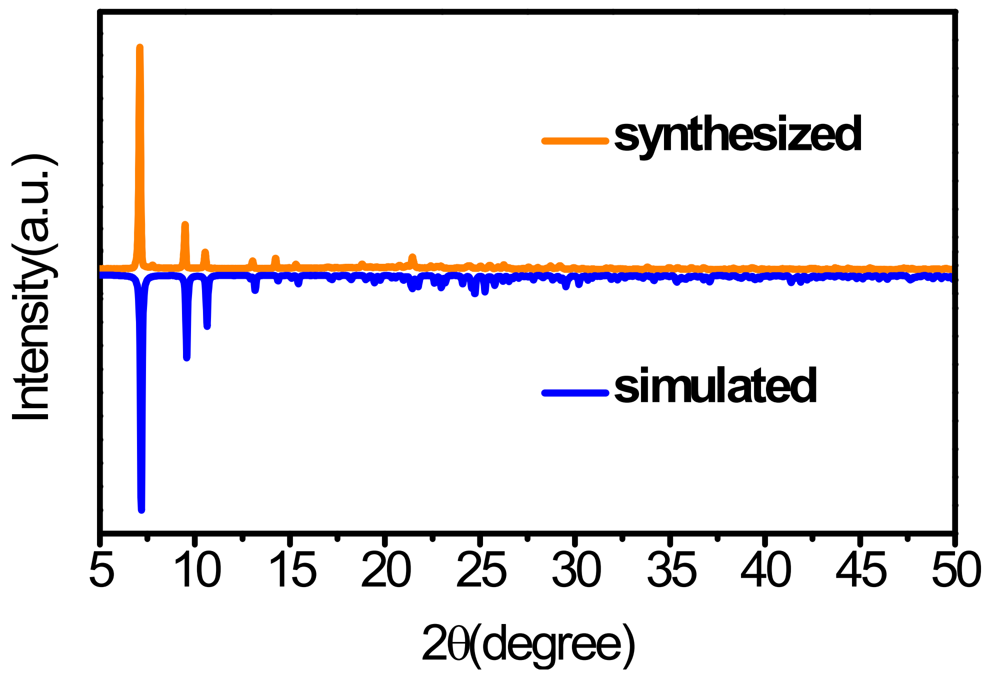

Figure S1. PXRD patterns of $\mathbf{Cu_nI_n(PNP)_{n/2}}$ and corresponding simulated one from single crystal.

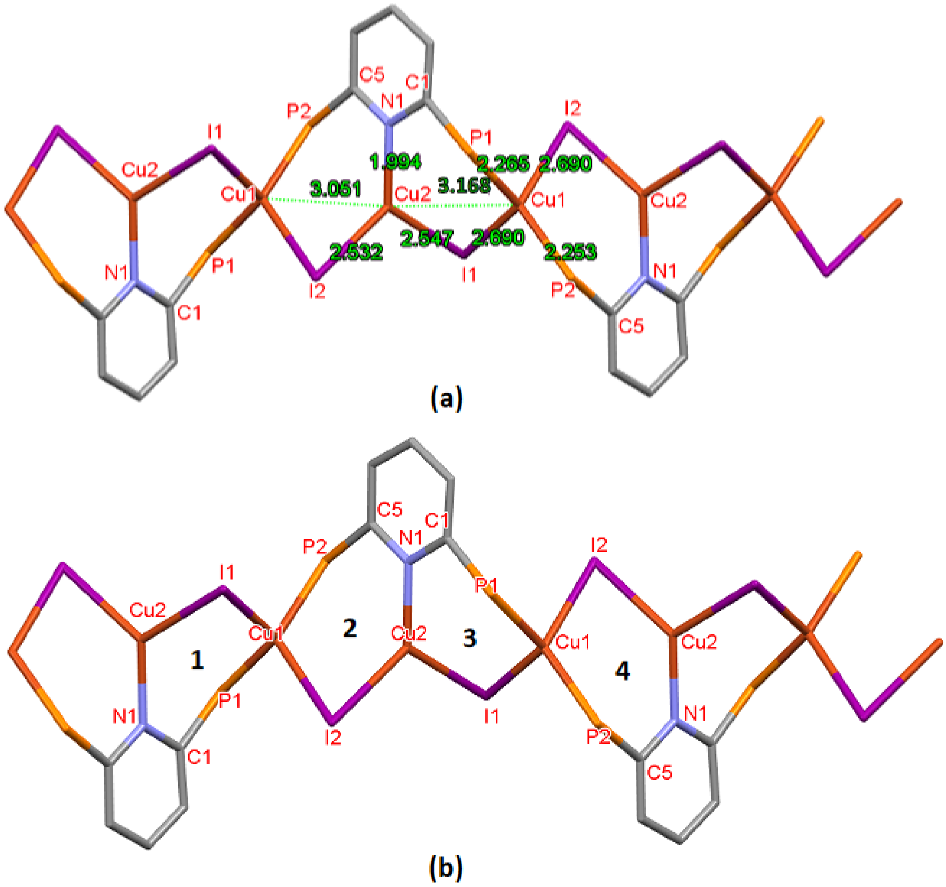

Figure S2. View of 1D structural diagram towards b axis of $\mathbf{Cu_nI_n(PNP)_{n/2}}$, showing (a) Cu···Cu and Cu-X (X=P, N ,I) bond length, and (b) Six-membered ring.

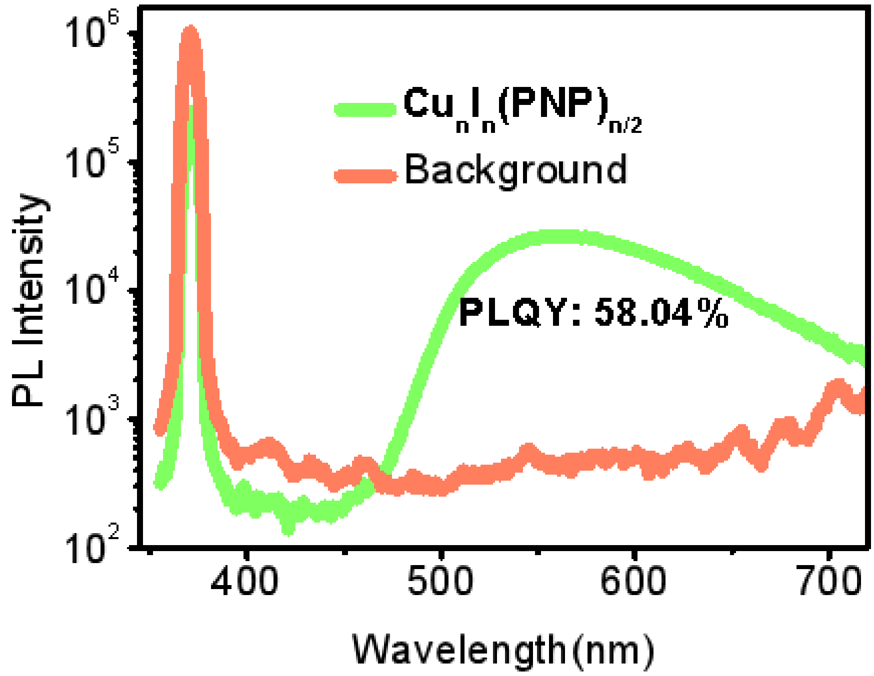

(a)

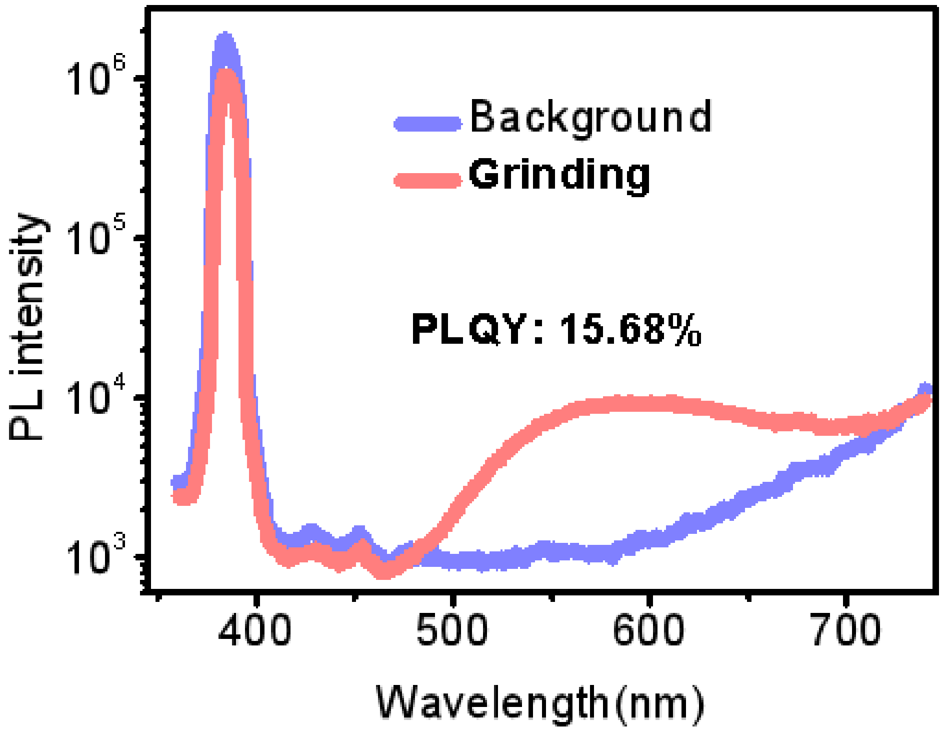

(b)

Figure S3. The PLQY of (a) $\mathbf{Cu_nI_n(PNP)_{n/2}}$ crystals and (b) corresponding grinding powder of $\mathbf{Cu_nI_n(PNP)_{n/2}}$ crystals.

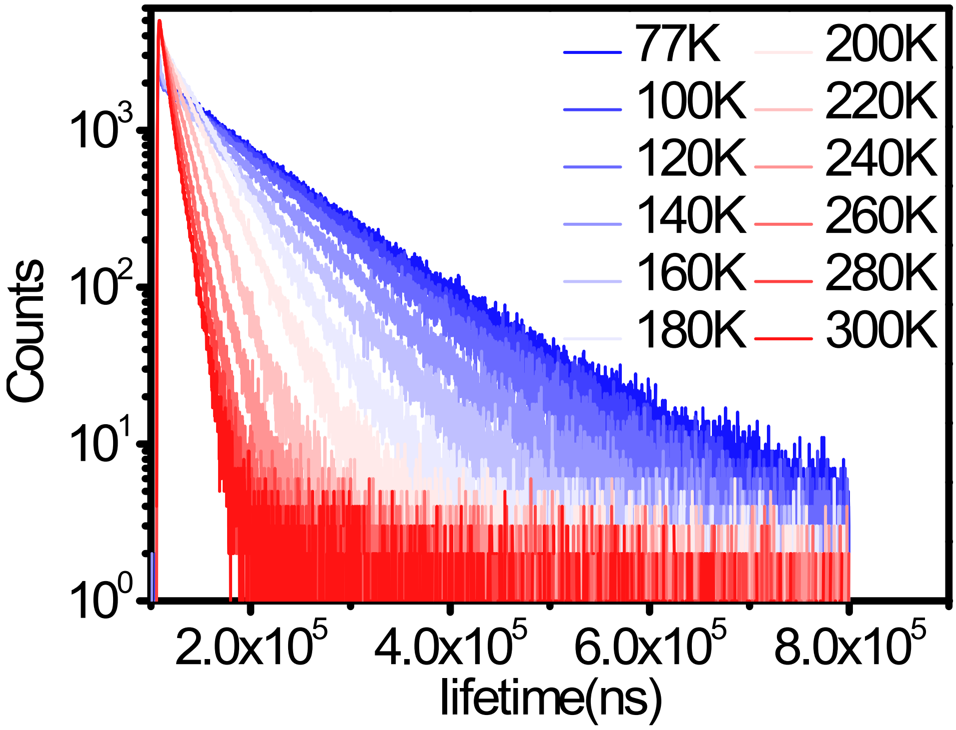

Figure S4. Emission decay time curves of **$Cu_nI_n(PNP)_{n/2}$** monitored at 546 nm under excited at **375** nm at various temperature ranging from 77-300 K.

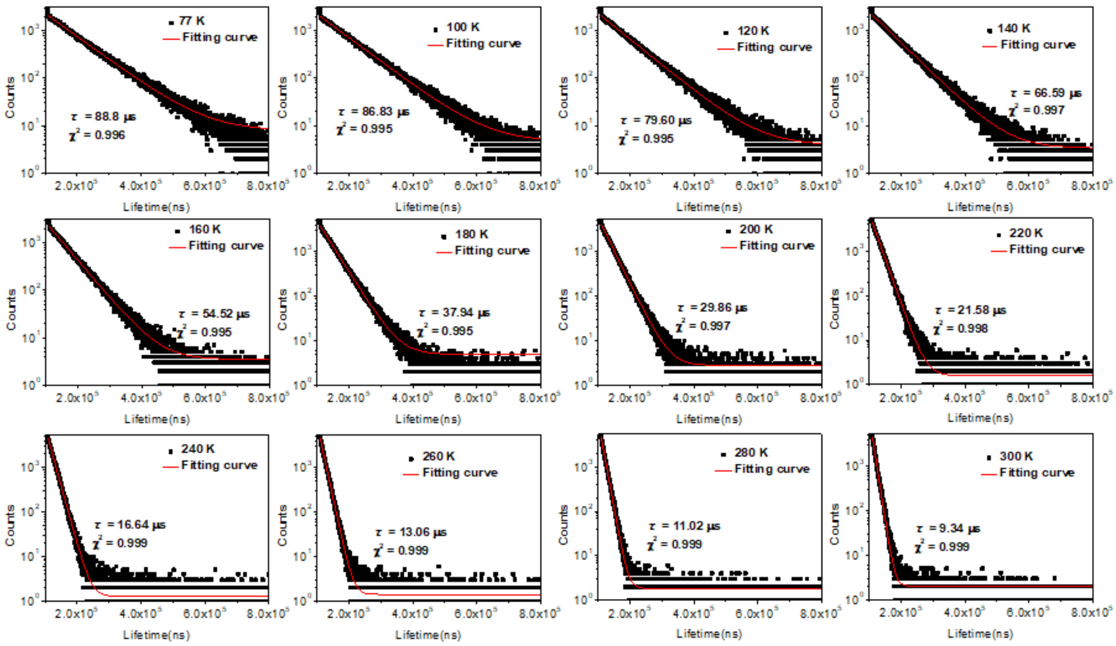

Figure S5. Emission decay time curves of **$Cu_nI_n(PNP)_{n/2}$** monitoring at 546 nm under excited at **375** nm at various temperature ranging from 77-300 K.

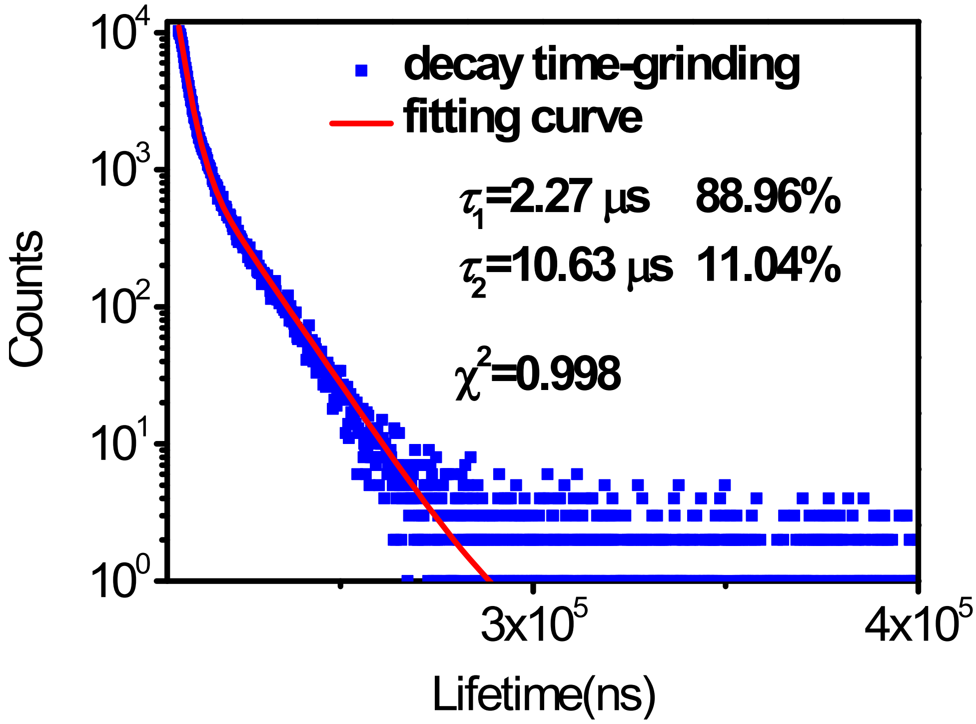

Figure S6. Emission decay time curve of grinding $\mathbf{Cu_nI_n(PNP)_{n/2}}$ monitoring at 590 nm under excited at **375** nm.

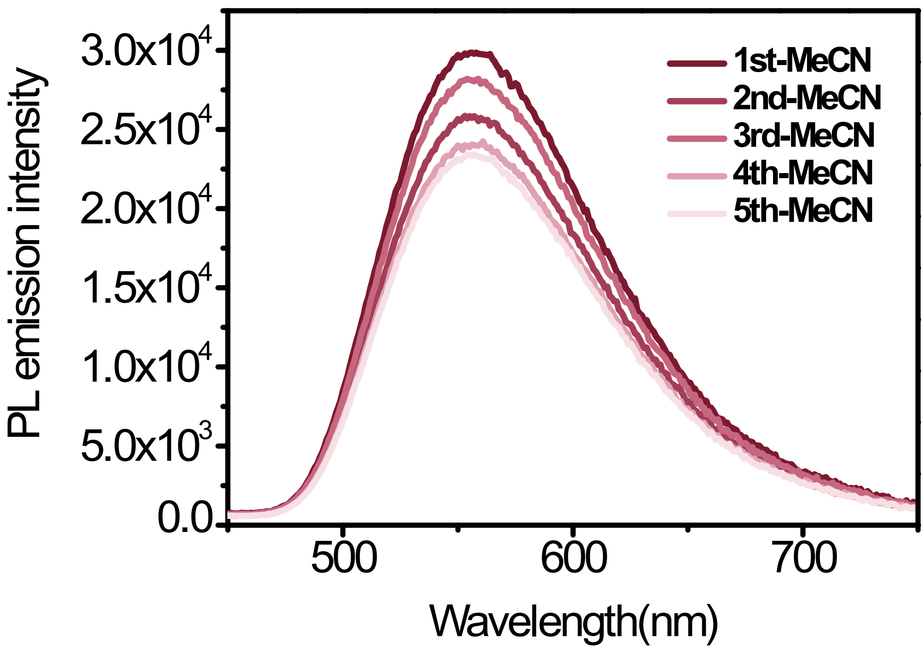

(a)

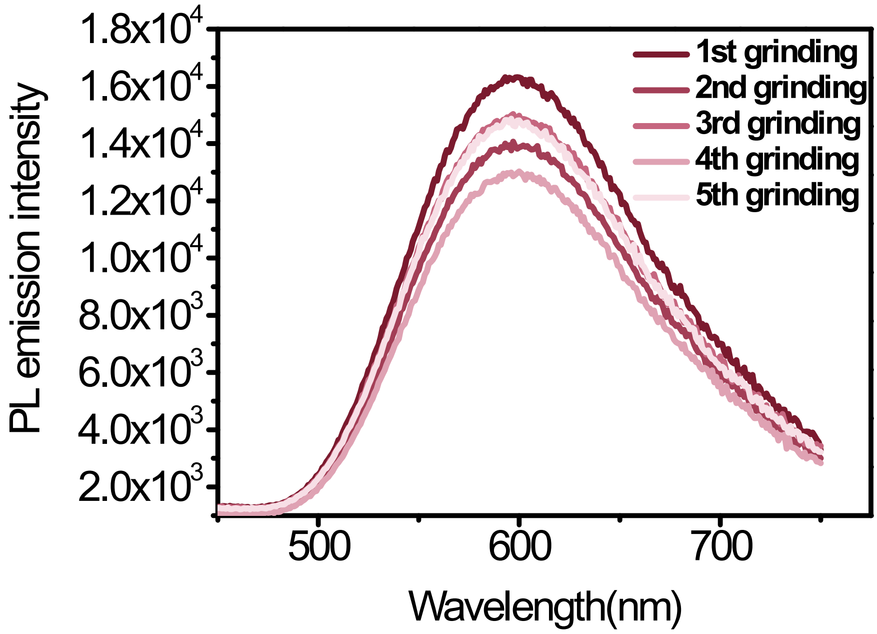

(b)

Figure S7. The PL emission spectra of reversible process involving (a) MeCN treatment and (b) grinding after multiple cycles.

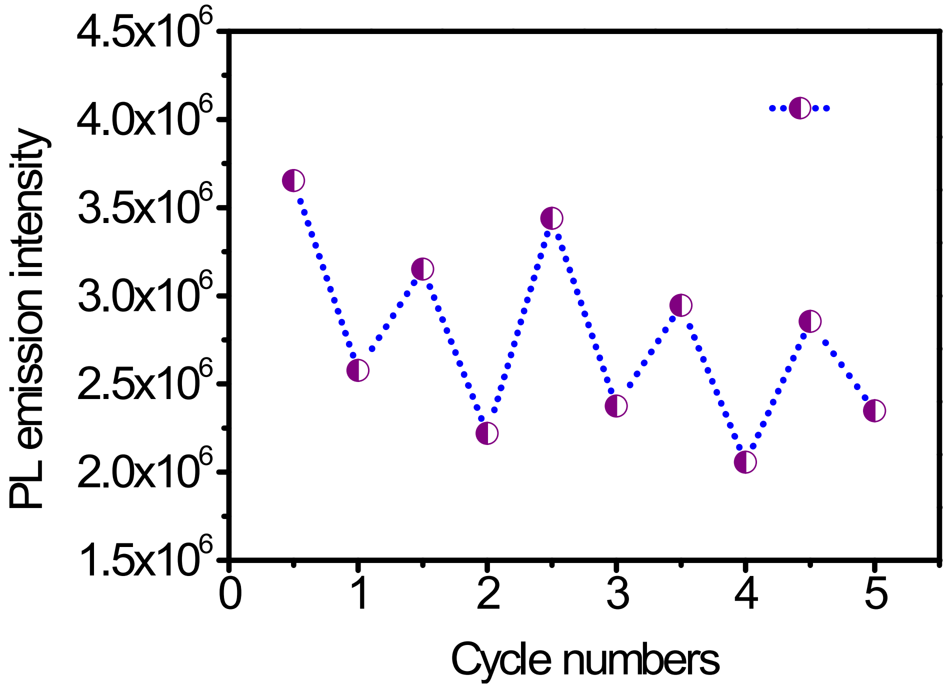

Figure S8. The PL emission intensity of reversible process involving (a) MeCN treatment and (b) grinding after multiple cycles.

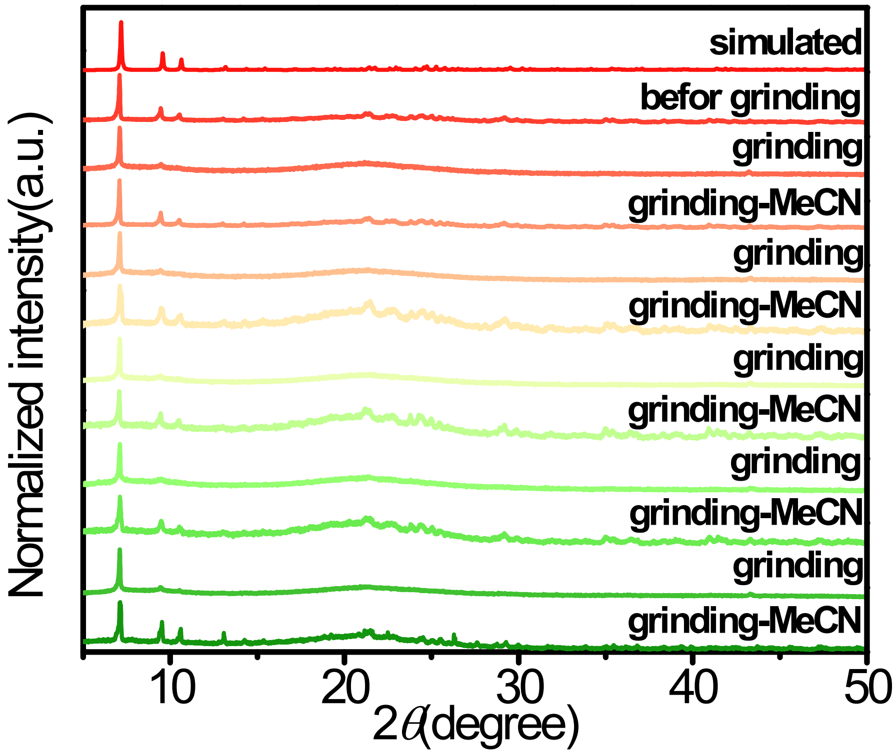

Figure S9. The PXRD patterns of reversible process involving (a) MeCN treatment and (b) grinding after multiple cycles.

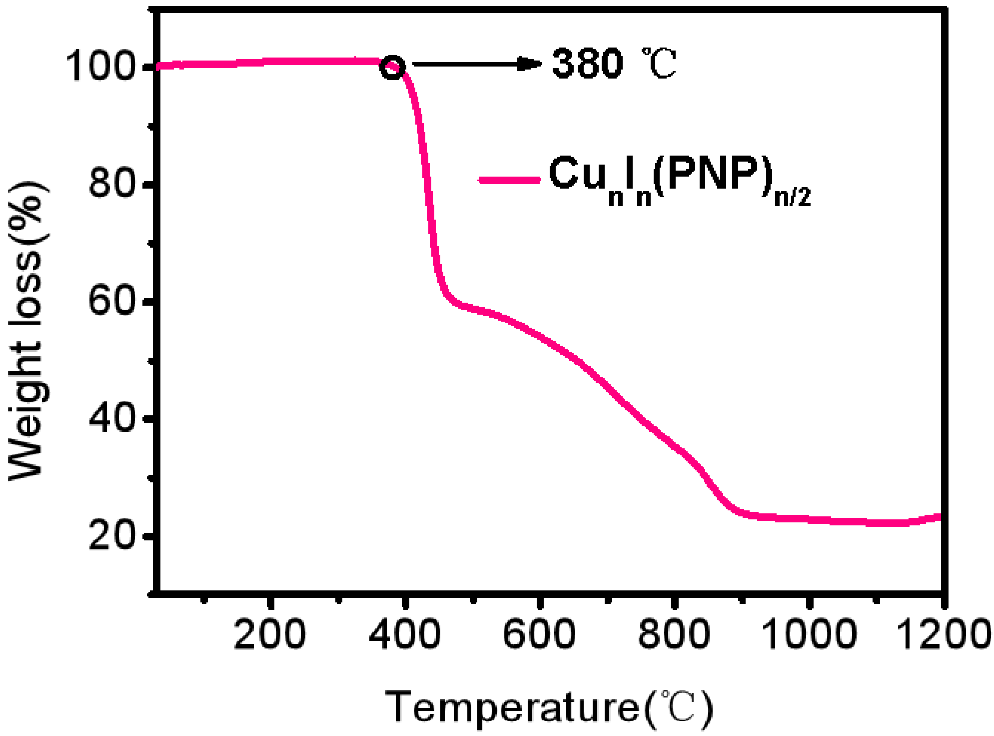

Figure S10. TGA curve of $\mathbf{Cu_nI_n(PNP)_{n/2}}$ in the range of 30-1200°C.

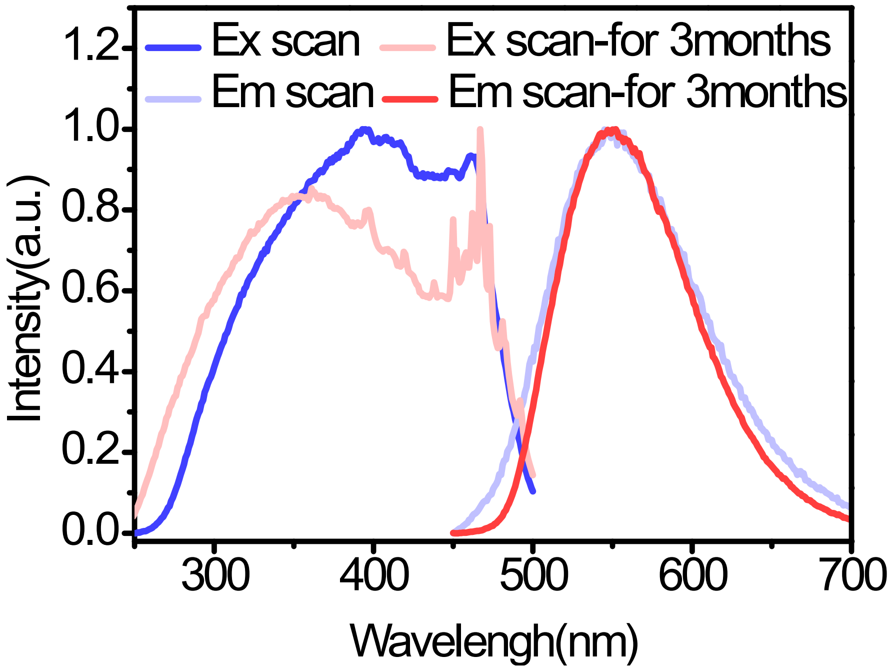

Figure S11. PL and PLE spectra of original $\mathbf{Cu_nI_n(PNP)_{n/2}}$ and corresponding one exposed in air condition for 3 months.

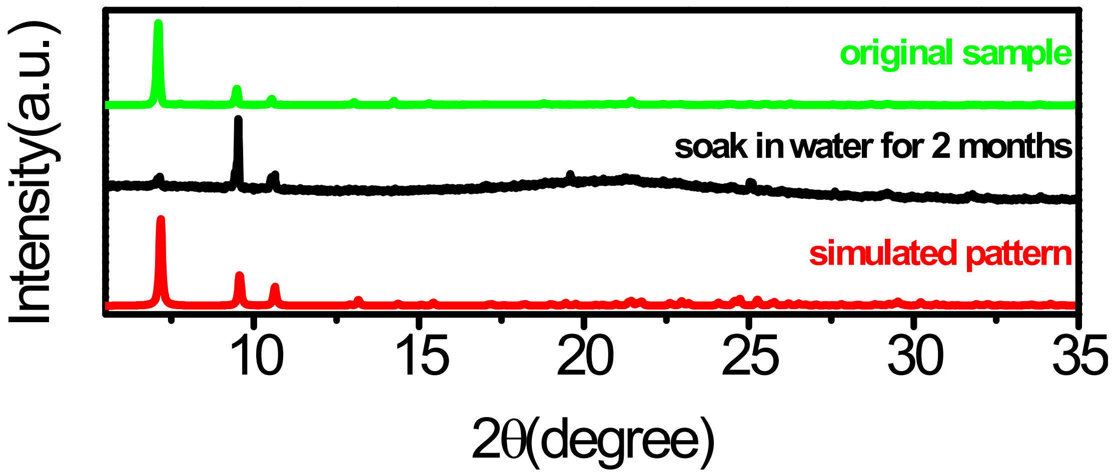

Figure S12. PXRD patterns of original $\mathbf{Cu_nI_n(PNP)_{n/2}}$ and corresponding sample soaked in water for 2 months.

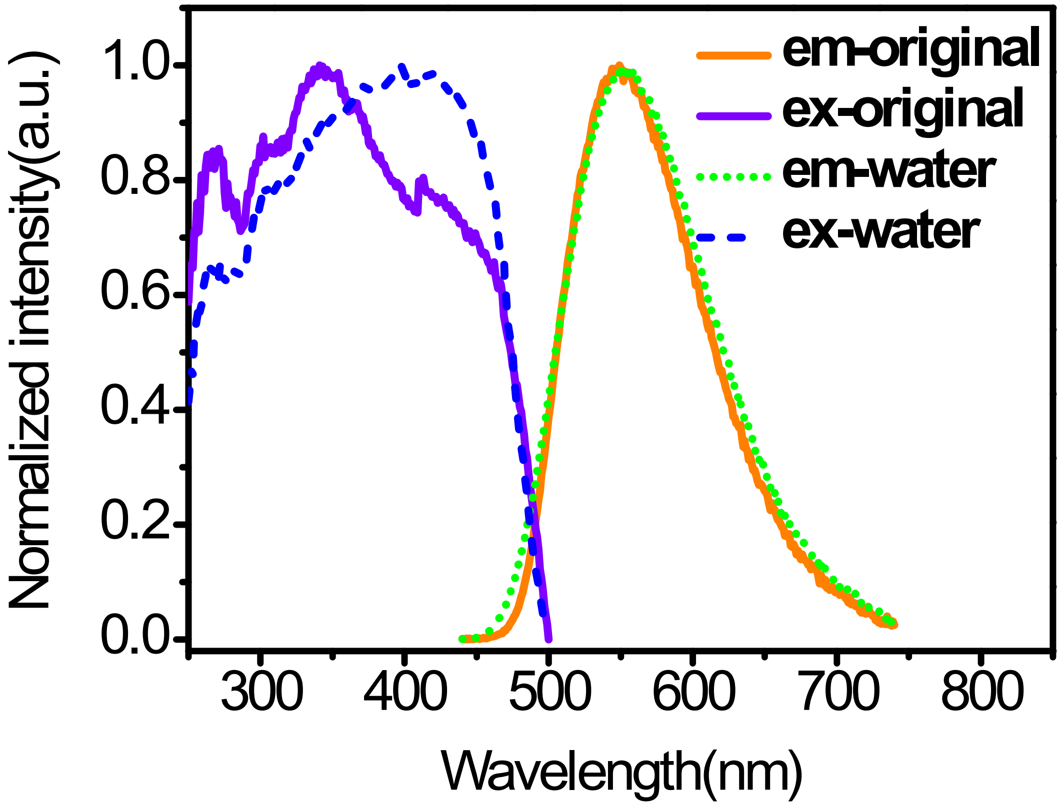

Figure S13. PL and PLE spectra of original $\mathbf{Cu_nI_n(PNP)_{n/2}}$ and corresponding sample soaked in water for 2 months.

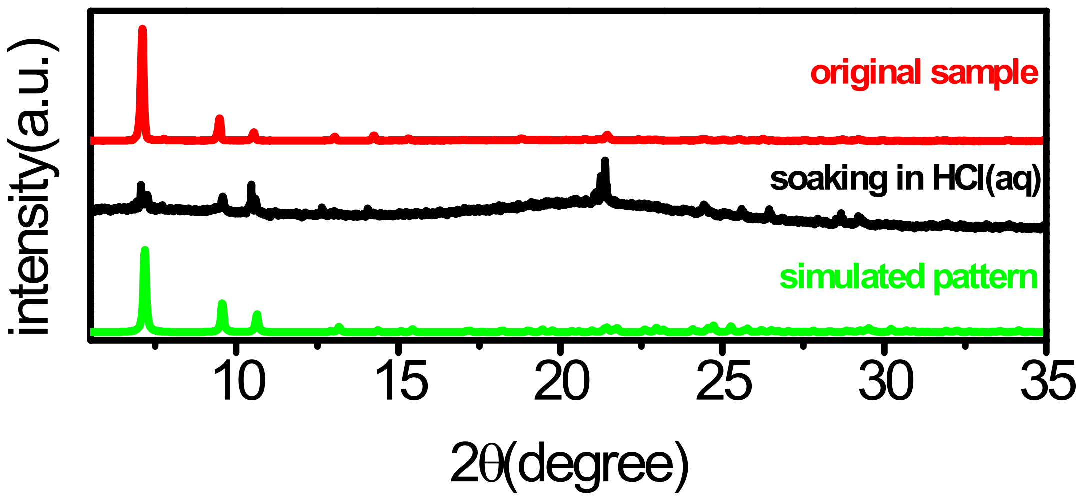

Figure S14. PXRD patterns of original $\mathbf{Cu_nI_n(PNP)_{n/2}}$ and corresponding sample soaked in hydrochloric acid for 6 hours.

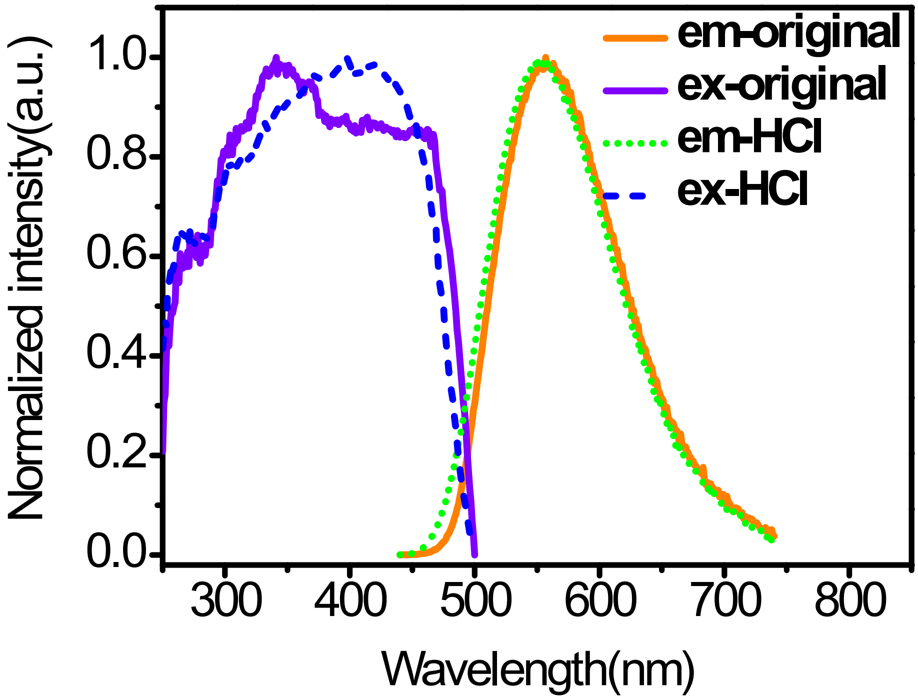

Figure S15. PL and PLE spectra of original $\mathbf{Cu_nI_n(PNP)_{n/2}}$ and corresponding sample soaked in hydrochloric acid for 6 hours.

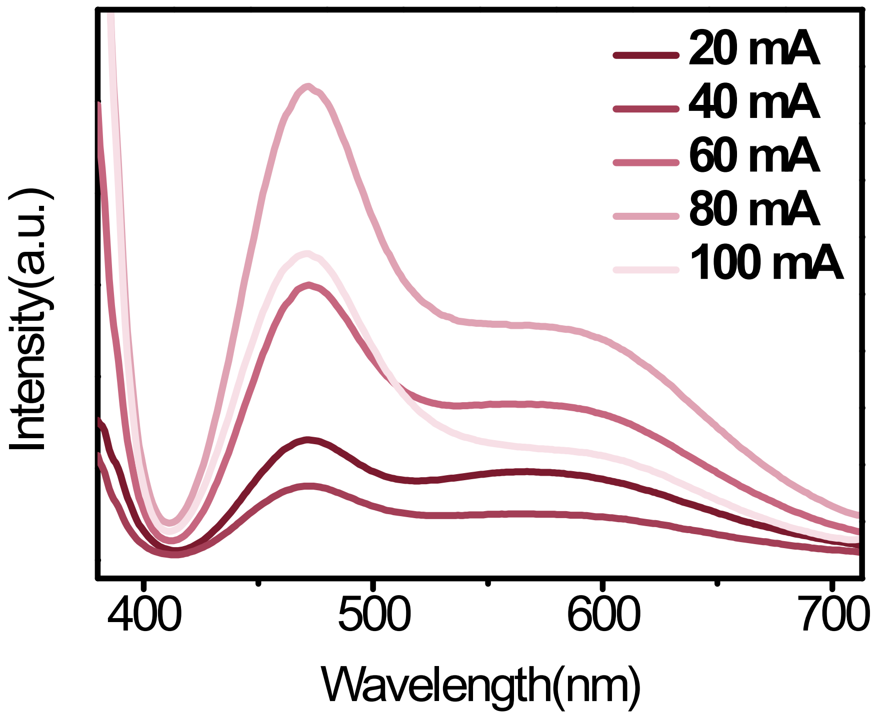

Figure S16. The spectrum under different current density (20-100 mA).

Table S1. Single X-Ray Diffraction Crystallographic Data of **$Cu_nI_n(PNP)_{n/2}$**.

Compounds	**$Cu_nI_n(PNP)_{n/2}$**
Moiety formula	$C_{29}H_{23}Cu_2I_2NP_2$
Formula weight / $g.mol^{-1}$	828.32
Temperature / K	298
Crystal system	Monoclinic
Space group	$P2_1/n$
a **/ Å**	14.021(3)
b **/ Å**	12.077(2)
c **/ Å**	17.349(4)
α **/ deg**	90
β **/ deg**	106.63(3)
γ **/ deg**	90
volume / $Å^3$	2814.9(10)
Z	4
ρ_{calc} / $g.cm^{-3}$	1.955
***F*(000)**	1592.0
Crystal size / mm^3	0.16 × 0.18 × 0.37
μ / mm^{-1}	3.838
Radiation	Mo Kα (λ = 0.71073 Å)
Final *R* indexes [all data]	R_1^a =0.0484 wR_2^b=0.1202
GOF	1.030

(a) $R_1 = \sum \left| F_o - F_c \right| / \sum F_o$

(b) $wR_2 = \sum \left[w(F_o^2 - F_c^2)^2 / \sum \left[w(F_o)^2 \right] \right]^{1/2}$

Table S2. Selected bond angle (°) of $\mathbf{Cu_nI_n(PNP)_{n/2}}$.

	Atom1	Atom2	Atom3	Bond angle
1	I1	Cu1	I2	95.29(3)
2	I1	Cu1	P1	118.61(5)
3	I1	Cu1	P2	101.58(5)
4	I2	Cu1	P1	101.33(5)
5	I2	Cu1	P2	120.60(5)
6	P1	Cu1	P2	118.12(7)
7	I1′	Cu2	I2	110.67(4)
8	I1′	Cu2	N1	122.0(2)
9	I2	Cu2	N1	127.4(2)
10	Cu2	I1	Cu1′	74.40(3)
11	Cu1	I2	Cu2	71.42(3)

Table S3. Selected bond length (Å) of $\mathbf{Cu_nI_n(PNP)_{n/2}}$.

	Atom1	Atom2	Bond length
1	Cu1	I1	2.690(1)
2	Cu1	I2	2.690(1)
3	Cu1	P1	2.265(2)
4	Cu1	P2	2.253(2)
5	Cu2	I1	2.547(1)
6	Cu2	I2	2.532(1)
7	Cu2	N1	1.994(5)
8	Cu2	Cu1	3.168(1)
9	Cu1′	Cu2	3.051(1)

Table S4. The emission decay time of $Cu_nI_n(PNP)_{n/2}$ at various temperature ranging from 77-300 K.

	Temperature/K	**Lifetime/μs**
1	77	88.8
2	100	86.83
3	120	79.6
4	140	66.6
5	160	54.52
6	180	37.94
7	200	29.86
8	220	21.58
9	240	16.64
10	260	13.06
11	280	11.02
12	300	9.34

Table S5. Vertical excitation energies ($S_1 \leftarrow S_0$ and $T_1 \leftarrow S_0$, in eV) and associated singlet-triplet energy gap (ΔE_{ST}) calculated with TD-DFT method.

compound	$S_1 \leftarrow S_0$	$T_1 \leftarrow S_0$	ΔE_{ST}(eV)
$Cu_nI_n(PNP)_{n/2}$	0.228	0.108	0.12

Table S6. The percentage of Phosp. and TADF in total intensity $I_{tot} = I(S_1) + I(T_1)$ of a diversity of copper(I) complexes.

Complex	Phosp. (%)+TADF(%)	Ref.
$Cu_nI_n(PNP)_{n/2}$	11+89	This work
1	32+68	1
2	41+59	1
3	33+67	1
$(PNNP)Cu_2I_2$	25+75	2
$[Cu(czpzpy)(PPh_3)]BF_4$	24+76	3

$Cu_4Cl_4(NP)_2$	48+52	4

References

[1]. G. Farias, C. A. M. Salla, J. Toigo, L. Duarte, A. J. Bortoluzzi, E. Girotto, H. Gallardo, T. D. Z. Atvars, B. de Souza and I. H. Bechtold, *Dalton Trans.*, 2022, **51**, 1008-1018.

[2]. J. H. Jia, X. L. Chen, J. Z. Liao, D. Liang, M. X. Yang, R. Yu and C. Z. Lu, *Dalton Trans.*, 2019, **48**, 1418-1426.

[3]. X.-L. Chen, C.-S. Lin, X.-Y. Wu, R. Yu, T. Teng, Q.-K. Zhang, Q. Zhang, W.-B. Yang and C.-Z. Lu, *J. Mater. Chem. C*, 2015, **3**, 1187-1195.

[4]. X. L. Chen, R. Yu, X. Y. Wu, D. Liang, J. H. Jia and C. Z. Lu, *Chem. Commun.*, 2016, **52**, 6288-6291.